ELSEVIER

Journal of Supercritical Fluids 22 (2002) 21–36

THE JOURNAL OF Supercritical Fluids

www.elsevier.com/locate/supflu

Determination of the solubility of extracts from vegetable raw material in pressurized CO_2: a pseudo-ternary mixture formed by cellulosic structure + solute + solvent

Vera M. Rodrigues [a], Elisa M.B.D. Sousa [b], Alcilene R. Monteiro [c], Osvaldo Chiavone-Filho [b], Marcia O.M. Marques [d], M. Angela A. Meireles [a,*]

[a] *LASEFI–DEA/FEA–UNICAMP, ntos, Cx. Postal 6121, CEP: 13083-970, Campinas SP, Brazil*
[b] *DEQ–UFRN, Campus Universitário s/n-Núcleo Tecnológico/PPGEQ, Lagoa Nova CEP: 59072-970, Natal RN, Brazil*
[c] *CCTA–UENF, Av. Alberto Lamego, 2.000, Horto 28.015-620, Campos do Goytacazes RJ, Brazil*
[d] *IAC–Cx. Postal 28, CEP: 13001-970, Campinas SP, Brazil*

Received 3 April 2001; received in revised form 1 August 2001; accepted 24 August 2001

Abstract

This paper discusses the application of the dynamic method to measure the solubility in pseudo-ternary systems formed by vegetable raw materials (cellulosic structure + solute) and CO_2. For aromatic, medicinal, and spice plants, the soluble portion of the solid is formed of essential oils, oleoresins, pigments, and various substances from several other classes of organic compounds. The experimental data were measured in two independent laboratories, using three experimental set-ups, and three vegetable species: clove buds, eucalyptus, and ginger. The solubility for the system clove buds/CO_2 varied from 0.220 to 0.277 kg-extract/kg-CO_2 for the isotherm of 288.15 K. The ginger extract solubility varied from 2.01×10^{-3} to 7.20×10^{-3} kg-extract/kg-CO_2 for pressures of 100–300 bar, and temperatures of 298.15–313.15 K. The eucalyptus solubility for the isobar of 66.7 bar varied from 3.95×10^{-3} to 4.07×10^{-3} kg-extract/kg-CO_2. © 2002 Elsevier Science B.V. All rights reserved.

Keywords: Solubility; SFE; Clove buds; Ginger; Eucalyptus

Nomenclature

d_a	apparent density of the bed, kg/m^3
D_{aY}	axial dispersion coefficient
d_r	real or true density of bed and particles, kg/m^3
H	measuring-cell length, m

* Corresponding author. Tel.: +55-19-3788-4033; fax: +55-19-3788-4027.
E-mail address: meireles@ceres.fea.unicamp.br (M.A.A. Meireles).

0896-8446/02/$ - see front matter © 2002 Elsevier Science B.V. All rights reserved.
PII: S0896-8446(01)00108-5

$J(X, Y)$	interfacial mass transfer rate, kg solute/s.kg cellulosic structure
M^*	mass transfer rate for the CER period for Q^*, kg solute/s
M_{CER}	mass transfer rate for the constant extraction rate period, kg solute/s
Q^*	solvent flow rate suitable for solubility measurement, kg CO_2/s
t	time, s
t_{CER}	duration of the constant extraction rate period, s
t^*	duration of the CER period for Q^*, s
u	interstitial velocity, m/s
u^*	interstitial velocity suitable to solubility measurement, m/s
X	mass ratio of solute in solid phase, kg solute/kg cellulosic structure
Y^*	solubility, kg solute/kg solvent
Y	mass ratio of solute in solvent phase, kg solute/kg of solvent
Y_{CER}	mass ratio of solute in solvent phase at measuring-cell outlet, kg solute/kg solvent
Z	axial direction, m

Greek symbols

ε	porosity of the bed and particles

1. Introduction

The increasing use of vegetable extracts by the food, cosmetic, and pharmaceutical industries can make the SFE of essential oils using supercritical carbon dioxide (CO_2) a very attractive technology compared to conventional processes with respect to the product quality. The knowledge of the mass transfer mechanisms, the kinetics parameters and the thermodynamics restrictions of the extraction conducted in a bed of vegetable material can clear up the scenario to make the process economically viable. This requires information on the thermodynamic restrictions of the system vegetable material/CO_2. On the other hand, the understanding of the various process variables and how they can be connected to a theoretical model to describe the extraction kinetics are also desirable. The aim of this paper is to discuss and present experimental data for the solubility of systems such as vegetable material/CO_2. Experimental data were measured for clove buds/CO_2, eucalyptus/CO_2, and ginger/CO_2.

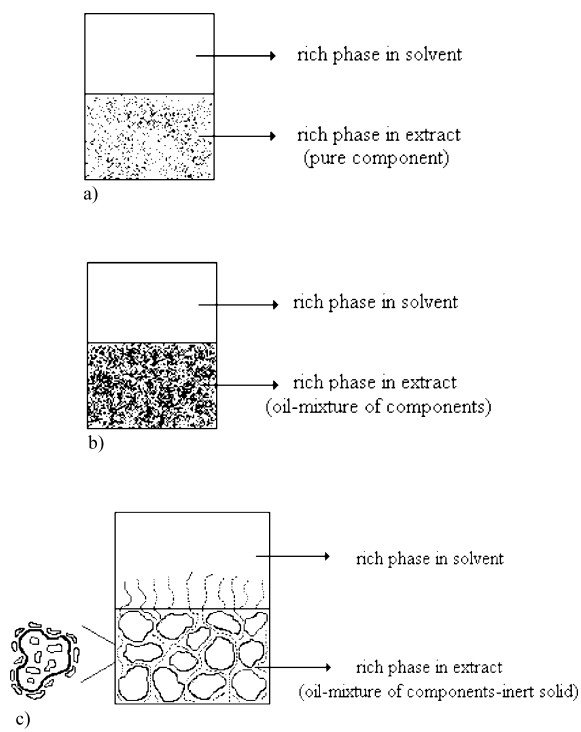

Fig. 1. Illustration for: (a) binary system; (b) pseudo-binary system; (c) pseudo-ternary system.

1.1. Pseudo-ternary system definition

For SFE from solid substratum, the system vegetable material + CO_2 can be pictured as being formed of three components: solvent, extract or solute, and cellulosic structure. The cellulosic structure can be considered completely inert to the solvent (CO_2) but it strongly interacts with the extract or the solute. For odoriferous, medicinal, and spice plants, the soluble portion of the solid substratum is formed of essential oils, oleoresins, pigments, and various substances from several classes of organic compounds. The extract is then a complex mixture of chemical species such as terpenes, terpenoids, oxygenated and non-oxygenated phenyl propanoid derivatives, and other compounds such as esters, etc. and so the solute is formed by a multicomponent mixture. Fig. 1 illustrates three situations that may be present in SFE process: Fig. 1a shows the situation for a system formed by a pure component + CO_2. If instead of a pure component the solute is a multicomponent mixture such as the clove volatile oil, then the system can be approximated by a pseudo-binary system as in Fig. 1b. On the other hand, because of the presence of the solid substratum, the system is composed of cellulosic structure + solute (multicomponent mixture) + solvent (CO_2), so that a very simplified picture of the system is to treat it as a pseudo-ternary system (Fig. 1c). In general, the solute in the solid substratum is located inside cells and specialized structures that may or may not suffer rupture when subjected to a pre-treatment (milling) to favor mass transfer of the solute to the fluid phase. For the system solid substratum + CO_2, the cellulosic structure does not modify in the presence of the solvent, that is, the cellulosic structure remains inert to the solvent during the extraction process, while the solute strongly interacts with both the solvent and the cellulosic structure. However, as will be shown, the solubility is not a very strong function of the raw material origin and this can possibly be overlooked for design purposes.

The present work describes the influence of the cellulosic structure over the solubility of the extract in the CO_2, where the solubility is defined for a pseudo-ternary system. A good discussion about the influence of the cellulosic structure on the solubility for vegetable materials/CO_2 systems is given by Brunner [1]. This author also demonstrated that the solubility of pure caffeine in CO_2 (binary system) is about 20 times larger than the solubility of the caffeine measured for the system coffee grains/CO_2 (pseudo-ternary system: cellulosic structure/solute/solvent). Considering all these facts and the need for information on the solubility of vegetable extracts in CO_2, particularly for aromatic, medicinal, and spice plants, the solubilities of the extracts of clove buds (*Eugenia caryophillus*), ginger (*Zingiber officinale* Roscoe), and eucalyptus (*Eucalyptus tereticornis*) in pressurized CO_2 were measured using the dynamic method [2]. The data were collected at two independent laboratories, using three equipments, the same experimental methodology and two calculation procedures.

2. Materials and methods

The procedure to measure solubility by the dynamic method resembles that of an extraction assay. Therefore, the experimental runs were conducted using SFE units. Three SFE units were selected and located at two laboratories: (i) LASEFI–DEA/FEA–UNICAMP (SFE_1 and SFE_3); and (ii) DEQ–UFRN (SFE_2). For every experimental condition, a series of runs with solvent flow rates from 0.28×10^{-5} to 3.2×10^{-5} kg/s was performed. Three plants were selected for the study because of their widespread use in food, cosmetics, and pharmaceutical industries. In addition, they have different agronomical profiles: clove (*E. caryophyllus*) is a large tree (up to 15 m) and the extract is obtained from its fruit; eucalyptus (*E. tereticornis* Smith) is a bunch and its extract is gotten from the leaves; ginger (*Z. officinale* Roscoe) is a rhizome. Assays with clove buds were performed at LASEFI–DEA/FEA–UNICAMP and DEQ–UFRN. The experiments with ginger were conducted at LASEFI and the ones with eucalyptus at DEQ–UFRN.

2.1. Raw material selected

2.1.1. Clove buds

Brazil is the second worldwide producer of clove buds. Clove buds or its oil are largely used in food processing, to impart flavor to cigarettes and cosmetics, and in other pharmaceuticals products [3]. Clove buds are a very important source of eugenol, a substance used in pharmaceutical products. In addition, eugenol is used for the synthesis of vanillin, eugenyl acetate, ethyl vanillin, and many other compounds [4].

2.1.2. Eucalyptus leaves

The *E. tereticornis* is easily cultivated in the Northeast of Brazil. Its leaves contain cineol or eucalyptol, the compound responsible for the astringent, balsamic, and anti-influenza activities. Its aroma resembles that of some preparations for bronchitis [5].

2.1.3. Ginger rhizomes

Ginger (*Z. officinale* Roscoe) is a plant of the Zingiberaceae family. It is originated mainly from tropical Asia and it has hundreds of different species, the genus 'zingiber' being the most significant as regards to cultivation for the Chinese people. It is also the most important root in the international market [6]. It possesses a soft spicy taste and a pleasant scent. Ginger and its extracts are used in food ingredients to improve their aroma and taste. It is also used by the pharmaceutical industry in medicines for colic reduction. Ginger is added to food in its natural form or as extract, essential oil or oleoresin. The essential oil, the volatile part of the rhizomes, is responsible for the aroma, generally obtained by steam distillation. The oleoresin, constituted of essential oil, resins and other non-volatile components, is generally obtained by extraction with organic solvent.

2.2. Raw material preparation

For the assays conducted at LASEFI–DEA/FEA–UNICAMP (Campinas, São Paulo, Brazil), the clove buds were bought at a local store (1997 crop), kept in plastic flasks hermetically closed, and stored in a domestic freezer (Brastemp, model vertical-750l, Brazil) at about 268.15 K. The amount of clove buds required for one experimental run was milled in a helix mill (Marconi, Model MA 345, Brazil). The system was kept at 289.15 K (PolyScience, model 9510, USA). The particle size distribution was measured using sieves of the Tyler series. Particles of sizes $-24/+48$ mesh were selected for the assays. For the assays performed at DEQ–UFRN (Natal, Rio Grande do Norte, Brazil), clove buds from Bahia (Brazil) were bought locally, and were cleaned, kept in plastic bags and stored in a domestic freezer (Consul, model 280, Brazil). For each assay, the frozen clove buds were triturated in a domestic food processor (Arno, model PRO, Brazil) for 15 min. The triturated material was separated using a sieve shaker (Produtest, no. 3614, Brazil) for 15 min. Equal amounts of particles of sizes $-20/+35$ and $-35/+48$ mesh were used.

The eucalyptus used was from the Experimental Station of the Federal University of Ceará (Horto de Plantas Medicinais, Fortaleza, Ceará, Brazil), and it was kept in plastic bags and stored in a domestic freezer (Consul, model 280, Brazil). For each assay, the frozen eucalyptus leaves were triturated in a domestic food processor (Arno, model PRO, Brazil) for 15 min. The triturated material was separated using a sieve shaker (Produtest, no. 3614, Brazil) for 15 min. Fifty percent of particles of sizes $-28/+35$, 25% of particles of sizes $-35/+48$ and 25% of $-20/+28$ mesh were used.

Gingers from two different crops were used. The first, denoted by Ginger_1, was from the first 1996 crop and purchased at Juquiá (São Paulo, Brazil). The second, denoted by Ginger_2, was harvested in September of 2000 and was from Atibaia (São Paulo, Brazil). Ginger_1 and Ginger_2 were stored and pre-treated in similar ways. The material was cleaned, selected, packed in plastic bags (10 or 5 kg) and stored in a domestic freezer (Metalfrio, Double-action, Brazil) at approximately 268.15 K. Ginger_1 was dried at low temperature (30 °C) using the procedure described by Monteiro et al. [7]. Ginger_2 was dried in the dryer described by Brod et al. [8] at 308.15 K (± 4 K). Particle size distribution was determined in a sieve shaker (Telastemp, Granutest, Brazil). The particles mean diameter was deter-

mined by the method of Gomide [9]. For all raw materials, the humidity was determined by the Jacobs' method [10].

2.3. Characteristics of the particles and of the fixed-bed

The fixed-bed apparent density (d_a) was calculated using the mass of solid, packed into the extractor (SFE_2) or into the extractor cell (SFE_1 and SFE_3), and its volume. The real or true density of the particles (d_r) was determined using a helium pycnometer at the Analytical Facilities of the Chemistry Institute—IQ/Unicamp. The porosity of the bed plus the particles was calculated as:

$$\varepsilon = 1 - \frac{d_a}{d_r}. \quad (1)$$

2.4. Experimental procedure

2.4.1. Measuring unit 1 (SFE_1)

The measuring unit SFE_1 is located at LASEFI–DEA/FEA–UNICAMP and was described by Rodrigues et al. [11]. The unit has an autoclave made of 316 LSS (Berghot, model HB-500, maximum pressure of 200 bar, Germany). The original heating system was substituted by a refrigerating jacket and the internal reservoir by a measuring-cell. The measuring-cell, made of Teflon, has a capacity of 0.5×10^{-3} m^3 with 0.064 m of diameter and 0.13 m of height. A cylindrical tube of Teflon (external diameter of 0.018 m, length of 0.144 m and wall thickness of 0.003 m) was adapted at the center of the measuring-cell. This device was used both as the extractor discharge line and as a thermocouple house (Ni–Cr/Ni–DIN 43710). At the upper end of the tube, a perforated lid with 0.064 m of diameter was adapted and used as a solvent distributor. At the bottom end of the tube, a 316 stainless steel filter (100 mesh) was placed to retain the fine solid particles dispersed in the mixture solute/solvent. The solid bed was formed inside the measuring-cell and had a concentric cylindrical shape. Shell and tube heat exchangers were used (316 stainless steel and length of 6 m) with nominal diameter of 1/4″ and of 1/8″. The system has a surge tank (White Martins Co., model 316 LSS DOF3A500, USA), with a jacket used both to control the solvent temperature and to eliminate pressure fluctuations at the extractor inlet. A HPLC pump (Thermoseparation Products, Model ConstaMetric 3200 P/F, USA) controlled the system pressure. The refrigerating bathes (PolyScience, model 9510, USA) used either water (extractor and surge tank) or a mixture of water and 90% of ethylene glycol (pump head) maintained at 263.15 K. The system also included a micrometering valve (Autoclave Engineering, model 10VRM 2812, USA); a digital flow meter ($\pm$0.02 l/min, Sierra Instruments Inc., USA); a flow totalizer ($\pm$0.02 l, LAO, model G-1, Brazil); a heating tape of 1.3 m (Fisaton, Brazil); a temperature sensor (Cole Palmer, model 0601-11, USA) with a controller (Dyna Sense, model 2156-40, USA); Bourbon type manometers ($\pm$1 bar, 100 and 250 bar, Record, Brazil); online filters (0.2, 0.6, and 20 μm, Swagelok, model SSF-4F, TF N-986, USA); safety valves (400 bar, Swagelok, model 344-4B, serial E, USA); thermal insulation (Montemor, Brazil). The sample collectors were glass flasks of 2.0×10^{-5} m^3.

2.4.1.1. Experimental procedure for SFE_1. Two hundred grams or 180 g of milled clove buds were used for each experimental run. The refrigerating bathes were turned on and programmed to keep the temperature at 263.15 K. The system was pressurized up to the surge tank and the system allowed to reach constant temperature (3 h). Samples of the extract were collected every 5 min and weighted ($\pm$0.0001 g, Sartorious, model A200S, USA). The solvent flow rate was continuously monitored. For some runs, a glass column with 0.15 m of length and 0.006 m of diameter, containing adsorbent material (2×10^{-3} kg, Porapak Q, 80–100 mesh, Waters Associates Inc., USA), was placed at the solvent exit to measure the amount of light compounds eventually drained off with the solvent.

2.4.2. Measuring unit 2 (SFE_2)

The measuring unit SFE_2 is located at DEQ–UFRN and is similar to the unit described by

Ferreira et al. [12]. The unit has a carbon dioxide (99.5% purity, White Martins Gases Industriais) reservoir and a stainless steel surge tank of 500 cm^3 to refrigerate the solvent (liquid CO_2) to the desired temperature. The fixed-bed extractor consists of a stainless steel cylinder with 0.605 m of length and 0.0216 m of diameter (Brazil). The temperature was measured with a digital thermometer (Lutron, TM-905 model K, ± 0.1 °C). The system pressure was limited to 80 bar and monitored with pressure gauges (Record, with capacity for 100 ± 1 kgf/cm^2, Brazil). Details of SFE_2 can be found in Souza et al. [13].

2.4.2.1. Experimental procedure for SFE_2. The measuring-cell containing the particles was assembled into the SFE_2. The refrigerating system was turned on and the unit was allowed to reach the operating temperature and pressure. The valve located at the extractor's outlet was then opened. The zero time of the experiment was considered at the onset of the first drop of extract. Samples were collected every 20 min. The solvent flow rate was monitored every minute using both the flow totalizer (LAO, Mod G1, Brazil) and a soap-bubble flow meter.

2.4.3. Measuring unit 3 (SFE_3)

The measuring unit SFE_3 is also located at LASEFI–DEA/FEA–UNICAMP and was described by França and Meireles [14]. The unit has a carbon dioxide (99.9% purity, White Martins Gases Industriais) reservoir and stainless steel surge tanks refrigerated at 263.15 K (Polyscience, model 9510, USA) to keep CO_2 as a liquid. The CO_2 pump was from Thermoseparation Products (model 3200, USA). Inside the fixed-bed extractor (stainless steel, 0.43 m of length and 0.033 m of diameter, Brazil) the measuring-cell (stainless steel, 0.375 m of length and 0.0283 m of diameter, Brazil) was fitted, totally removable from the system. The temperature was measured with Fe–Constantan thermocouples adapted to a register (RobertShaw, model T4WM, UK). The pressure was monitored with pressure gauges (Terbrasma, model 2541, 0–100 bar, ± 1 bar, Brazil and Record, model 1554, 0–500 bar, ± 0.5 bar, Brazil).

2.4.3.1. Experimental procedure for SFE_3. Eighty grams of dry ginger, containing equal amounts of particles of sizes 14, 16 and 24 mesh, were manually packed in the measuring-cell. About 2 g of the sample were placed per time, with the aid of a funnel and of a metallic stem of 1/4″ of diameter, in a way to avoid the deformation and breakage of the solid material. The measuring-cell was then adapted to the extractor column. The relief valves of the entrance and exit of the extractor and the pump valve were opened up. After this, the pump was turned on to pressurize the extraction line. The pressurization of the tubing was accomplished in several steps. First, the system was pressurized until the entrance of the extraction column. When the operational conditions were reached, the inlet valve to the extraction column was opened up and the measuring-cell was pressurized. The valves after the extractor were kept closed. When the whole system was pressurized at the chosen conditions of pressure and temperature, the valves downstream the extractor were opened to begin the extraction. The extract samples were collected in glass flasks every 30 or 15 min. Immediately after the collector, a glass column (0.15 m of length and 0.08 m of diameter), with treated glass wool (Pyrex, model Filtering Fiber, USA) in its extremities and packed under vacuum with 65 mg of the polymeric porous Porapak Q (80–100 mesh, Supelco, lot 109, USA), was placed in order to retain the low molecular mass substances that could otherwise be drained with the solvent. After each sampling, the collector flask and the capture column were weighted and stored in a domestic freezer (Brastemp clean, Model 410, Brazil). Samples from the capture column are denoted by E1-CO_2 and that from the collector flasks as E2-CO_2. During the experimental run, the collector flask and the capture column were maintained in an ice-bath to avoid loss of the more volatile oleoresin components. The solvent flow rate was measured and monitored after expansion, for each sampling, by a soap-bubble flow meter [15], adapted in the exit of the solvent.

2.5. Chemical composition of the extract

The chemical composition of the clove extracts (SFE_1) was determined using a gas chromatograph (Shimadzu, model GC-17AF CBM 101, Japan) equipped with a capillary column DB-5 (30 m × 0.25 mm × 0.25 μm). The carrier gas was helium (1.7 ml/min). The temperature of the injector was 513.15 K and that of the detector 553.15 K. The temperature programming was 308.15 K (5 min), 308.15–528.15, 4 K/min, 528.15–553.15, 15 K/min and 553.15 K (10 min). Split ratio was 1/30 and the flow rate was 2.0 ml/min. The sample injected was 0.4 μl of extract diluted in ethyl acetate (0.005 g of extract diluted in 1.0 ml ethyl acetate, P. A., chromatographic grade, EM Science, lot 36079631). The identification of the substances was done by GCMS (Shimadzu, model QP-5000, Japan) using the GC conditions and was based on: (i) comparison of the substance mass spectrum with the GC-MS system data bank (Wiley 139 Library); (ii) comparison of the mass spectra with the data in literature [16]; and (iii) retention index [17]. The quantitative analysis of the extract employed the external standard method [18]. The quantification was done using a standard solution for each substance identified in the extract: Eugenol (P. A., Sigma, Lot: 17H0239), β-caryophyllene (P. A., Sigma, Lot: 38H2503), α-humulene (P. A., Sigma, Lot: 97H2505). The eugenyl acetate was obtained by acetylation of the eugenol using the method described by Matos [19]. The clove extracts from SFE_2 were analyzed using a gas chromatograph (Varian, Model Star 3400 CX, USA) equipped with a capillary column DB-5 (30 m × 0.32 mm × 0.25 μm). The carrier gas was nitrogen (1.4 ml/min). The temperature of the injector was 523.15 K and that of the detector 593.15 K. The temperature programming was 308.15–453.15 K, 4 K/min, and 453.15–471.15 K, 2 K/min. The identification of the substances was done by GCMS (HP–5890 series II and 5911A) using the GC conditions and was based on: (i) comparison of the substance mass spectra with the GC-MS system data bank (Wiley 139 Library); (ii) comparison of the mass spectra with the data in literature [16]; and (iii) retention index [17].

The ginger extracts were analyzed using a GCMS system (Shimadzu, model QP-5000, Japan) equipped with a fused silica capillary column DB-1 (25 m × 0.25 mm × 0.25 μm) (Ginger_1) and DB-5 (30 m × 0.25 mm × 0.25 μm) (Ginger_2). The electron impact technique (70 eV) was used. The carrier gas was helium (1.7 ml/min) and 1 μl of sample was injected. The temperature was held at 323.15 K for 5 min and then raised to 553.15 K at 5 K/min. The detector temperature was 503.15 K and that for the injector was 513.15 K. The identification of the chemical constituents was based on: (i) comparison of the substance mass spectra with the GC-MS system data bank (Wiley 139 Library); (ii) comparison of the mass spectra with the data in literature [16]; and (iii) retention indexes [17].

The chemical composition of the eucalyptus extract was determined using the same equipment and identification methodology previously described for the clove extract (SFE_1). The carrier gas was helium (1.0 ml/min). The temperatures of the injector and of the detector were 423 and 303 K, respectively. The temperature programming was 333–513 K, 3 K/min.

2.6. Calculation procedures

Using the experimental data, the overall extraction curves (OEC) were fitted to a spline using two straight lines. The first line was identified with the constant extraction rate period (CER). From the spline, the extraction rate for the CER period (M_{CER}) was computed, as well as the time corresponding to the interception of the two lines (t_{CER}). The spline fit at LASEFI was done using the procedures PROC REG and PROC NLIN of SAS 6.12 [20]. For data obtained at DEQ–UFRN, the spline fitting was done using multiple-regression analysis (STATISTCA 5.0). MS Excel 97 was used to determine the interception of the two lines. The mass ratio of solute in the supercritical phase at the measuring-cell outlet (Y_{CER}) was obtained dividing M_{CER} by the mean solvent flow rate (Q_{CO_2}) for the CER period.

Table 1
Particle and bed characteristics

Raw material	Particle mesh	d_a kg/m^3	d_r kg/m^3	ε	Mean diameter $\times 10^3$, m
Clove (SFE_1)	24, 32, 48	526	1393	0.62	0.372
Clove (SFE_2)	35 and 48	864	1393	0.38	0.334
Ginger_1 and Ginger_2 (SFE_3)	14, 16, 24	400	1300	0.69	1.020
Eucalyptus (SFE_2)	28, 35, 48	546	1287	0.58	0.375

3. Results and discussions

Table 1 shows the characteristics of the fixed bed of the various raw materials. As can be observed, the real densities and the average particle diameter of clove buds and eucalyptus were very similar. The porosity of the bed for all systems was similar, except for the clove bud bed used in the SFE_2. Figs. 2–4 show the OECs and the spline used to describe the experimental data. The figures show that the spline fitting described quite well the experimental data. Therefore, the mass ratio of solute in the fluid phase at the measuring-cell outlet (Y_{CER}) for the three systems (SFE_1, SFE_2, and SFE_3) can be calculated by the procedure described previously using either SAS 6.12 or Statistica 5.0 and MS Excel 97.

As it is well known, any OEC will in general have a CER period that does not necessarily mean that the equilibrium was attained. Therefore, in order to measure the solubility for the ternary system using the dynamic method, a search for a suitable flow rate is required. The search must be performed for each measuring-cell geometry as well as for each temperature, pressure, and vegetable material. This way, in order to measure the solubility for the system vegetable material/CO_2, a series of experimental runs at different solvent flow rates for each temperature and pressure must be performed to identify the solvent flow rate at which the solvent leaves the measuring device saturated in solute. Fig. 5 shows the effect of the solvent flow rate on the mass ratio of solute in the supercritical phase at the measuring-cell outlet. The behaviors are the same regardless of the raw material and extraction unit used. The mass ratio of solute in the supercritical phase increases as the solvent flow rate increases

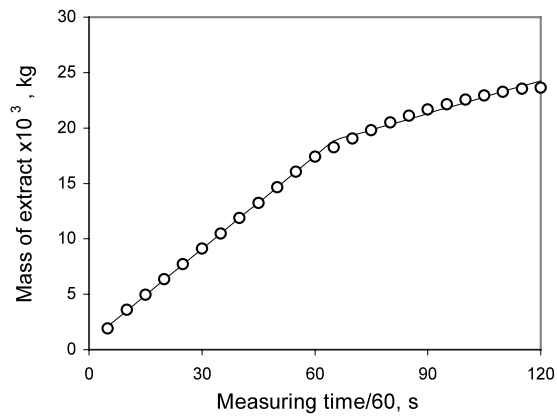

Fig. 2. Comparison between experimental data (○) and the spline (—) fitted using two straight lines at 288.15 K, 100 bar and 1.60×10^{-5} kg/s for clove (SFE_1).

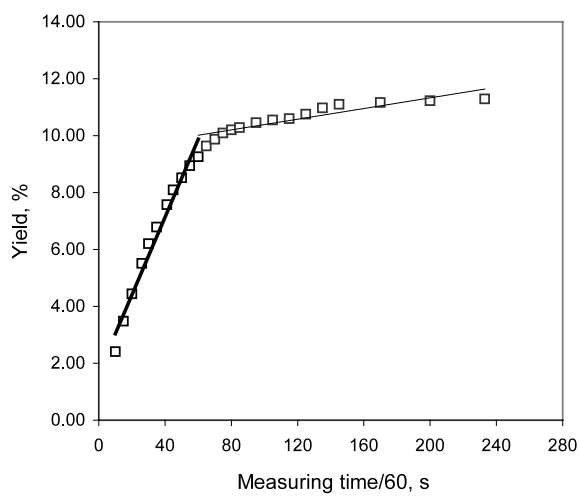

Fig. 3. Comparison between experimental data (□) and the spline (—) fitted using two straight lines at 288.15 K, 66.68 bar and 1.8482×10^{-5} kg/s for clove in SFE_2.

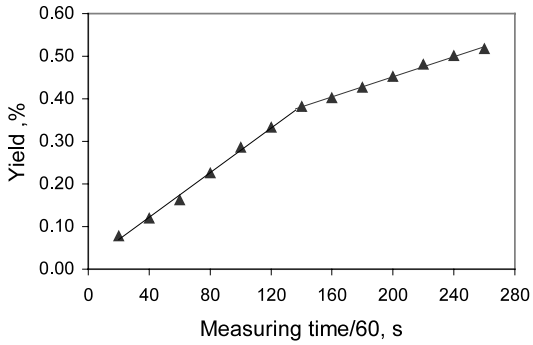

Fig. 4. Comparison between experimental data at 288.15 K, 66.68 bar, 1.30×10^{-5} kg/s (▲) and the spline fitting (-) for *E. tereticornis* (SFE_2).

up to a maximum, and decreases afterwards. At saturation, the solute mass ratio in the fluid phase at the bed outlet should be a maximum. Therefore, the solvent flow rate that is suitable to measure solubility is the value corresponding to this maximum. The maximum value of the Y_{CER} is identified with the solubility, Y^*, the corresponding solvent flow rate is denoted by Q^*, the velocity by u^*, the mass transfer rate by M^*, and the duration of the measuring period by t^*. For solvent flow rates larger than Q^*, the solvent leaves the system unsaturated while for values smaller than Q^* the axial dispersion may not be completely negligible. To get some insight into this phenomenon, let us consider the mass balance for the fluid phase for an element of the measuring-cell, with transfer in the axial direction only. We then have:

$$\frac{\partial Y}{\partial t} + u\frac{\partial Y}{\partial Z} = \frac{\partial}{\partial Z}\left[D_{aY}\frac{\partial Y}{\partial Z}\right] + \frac{J(X, Y)}{\varepsilon}, \quad (2)$$

where Y and X are the mass ratio of solute in the fluid and solid phase, respectively, t is time, u the interstitial velocity, Z the axial direction, D_{aY} the axial dispersion coefficient, ε the porosity, and $J(X, Y)$ the interfacial mass transfer rate. During the CER period, the mass ratio of solute remains constant with respect to time, and up to a certain value of the velocity the axial dispersion can be neglected, and so Eq. (2) can be simplified as [21]:

$$u\frac{\partial Y}{\partial Z} = \frac{J(X, Y)}{\varepsilon}. \quad (3)$$

Table 2 shows the order of magnitude of the axial dispersion term and the convective term as a function of the solvent flow rate. The coefficient of axial dispersion was estimated using the correlation of Butt (1980) cited by Santacessaria et al. [22]. Cathpole et al. [23] correlation was not used due to the range of temperature, pressure, and Reynolds number used to obtain the experimental data. The correlation of Tan and Liou [24] was avoided since it can produce deviations as high as 31% in the estimated value of the axial dispersion. From these results it is clearly seen that the importance of the axial dispersion term ($D_{aY}(\partial^2 Y/\partial Z^2) \approx D_{aY}(Y_{CER}/H^2)$) increases with the decrease in velocity. On the other hand, as the measuring-cell became shorter (SFE_1) the importance of the axial dispersion term relative to the convection one ($u(\partial Y/\partial Z) \approx u(Y_{CER}/H)$) increases. Therefore, in order to use the dynamic method to assess values of solubility for pseudo-ternary systems formed by vegetable material and supercritical fluid, it is necessary to experimentally determine Q^* (Fig. 5). The Y_{CER} data as a function of solvent flow rate were correlated using a second order polynomial. Comparing the polynomial fit of Fig. 5a and b for the system clove + CO_2, measured using SFE_1 and SFE_2, respectively, the following is observed: The second order polynomial correlated the data from SFE_2 better ($R^2 = 0.9897$) than the data from SFE_1 ($R^2 = 0.8596$). Considering that the ratio between the measuring-cell length to its diameter is ~ 2 for SFE_1 and ~ 28 for SFE_2, the results indicate that the most appropriate geometry for the measuring-cell is the one that keeps the ratio of the cell length to its diameter as big as experimentally convenient. Figs. 6–8 show the effects of raw material, temperature and pressure on the estimated value of the axial dispersion. The flow rates used for SFE_1 and SFE_2 were approximately the same, but due to the difference in geometry the velocities reached in SFE_2 were one order of magnitude larger than in SFE_1. Nonetheless, the importance of the axial dispersion term was bigger for SFE_1 as compared to either SFE_2 or SFE_3. Yet, in Fig. 6, it is interesting to notice that the influence of the system geometry (SFE_1 and SFE_2) is more pronounced than the effect

of the raw material (SFE_2: clove and eucalyptus). At 100 bar for the system clove + CO_2, the temperature did not affect the axial dispersion (Fig. 7). From Fig. 8 it can be seen that the pressure does not affect the general behavior of the axial dispersion term. The figure also illustrates the fact that the axial dispersion term increases with the increase in solvent flow rate and reaches a plateau. The beginning of this zone can be identified with the range of solvent flow rate suitable for solubility measurements, for the measuring-cell geometry and system operating conditions considered. Table 3 shows the measured solubility for the various raw materials. The values of Q^* and the corresponding experimental units are reported. As discussed before, for solvent flow rates larger than Q^* the solvent will leave the measuring-cell unsaturated. In addition, from the above discussion and the results of Fig. 5, if $Q_{CO_2} < Q^*$ the solvent will also leave the measuring-cell unsaturated due to the action of the axial dispersion. Then, for $Q_{CO_2} = Q^*$ and $t \leq t_{CER}$, Eq. (3) can be written as:

Table 2
Order of magnitude of the convective and axial dispersion terms of Eq. (2) as a function of the solvent flow rate

$Q_{CO_2} \times 10^5$ kg/s	$u \times 10^5$ m/s	$u(\partial Y/\partial Z) \approx [u(Y_{CER}/H)] \times 10^5$, kg/kg s	$D_{aY}(\partial^2 Y/\partial Z^2) \approx [D_{aY}(Y_{CER}/H^2)] \times 10^8$), kg/kg s
Clove: 100 *bar and* 298.15 *K* (*SFE*_1)			
1.30	0.92	1.69	12.87
1.47	1.04	1.95	14.83
1.65	1.16	2.39	18.17
1.70	1.20	2.47	18.73
1.92	1.35	2.48	18.78
2.15	1.52	2.43	18.43
2.70	1.91	2.82	21.36
Clove: 66.7 *bar and* 283.15 *K* (*SFE*_2)			
0.46	3.75	1.14	1.18
0.98	7.93	3.14	3.21
1.85	15.32	6.46	6.55
2.17	17.67	7.36	7.44
2.77	22.50	8.18	8.22
*Ginger*_1: 250 *bar and* 313.15 *K* (*SFE*_3)			
0.58	1.61	0.0006	0.006
1.30	3.58	0.0309	0.281
1.62	4.45	0.0526	0.475
2.12	5.83	0.0553	0.498
2.28	6.29	0.0434	0.390
2.50	6.89	0.0466	0.418
2.95	8.12	0.0542	0.484
*Ginger*_2: 100 *bar and* 313.15 *K* (*SFE*_3)			
1.70	6.80	0.0359	0.320
2.47	9.77	0.466	0.412
3.48	13.80	0.0589	0.514
Eucalyptus: 66.7 *bar and* 288.15 *K* (*SFE*_2)			
0.75	4.20	0.0208	0.049
1.30	7.27	0.0497	0.087
1.52	8.49	0.0559	0.098
1.95	10.90	0.6060	1.050
2.39	13.39	0.0403	0.069

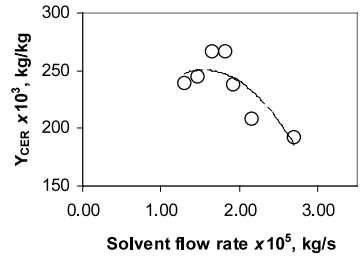

a. Clove at 100 bar, 298.15 K (SFE_1) ($R^2 = 0.8596$)

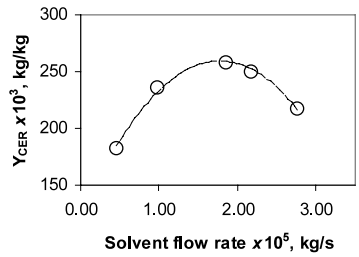

b. Clove at 66.68 bar, 283.15 K (SFE_2) ($R^2 = 0.9897$)

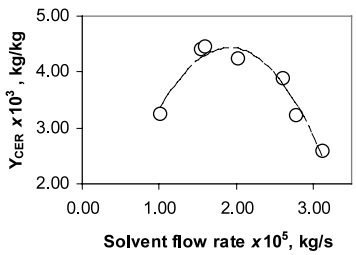

c. Ginger at 250 bar, 313.15 K (SFE_3) ($R^2 = 0.9452$)

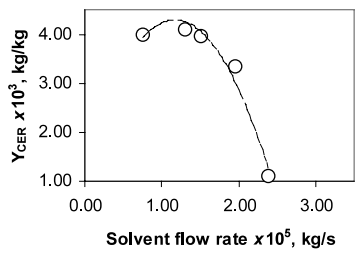

d. Eucalyptus at 66.68 bar, 288.15 K (SFE_2) ($R^2 = 0.9792$)

Fig. 5. Effect of solvent flow rate on the mass ratio of solute in the supercritical phase at the measuring-cell outlet. The line that represents the tendency lines for the experimental data are second order polynomial. R^2 is the correlation ratio.

$$u^* \frac{\partial Y}{\partial Z} = \frac{M^*}{N_{CO_2}}, \tag{4}$$

where N_{CO_2} is the mass of solvent used up to time t^*. Integration of Eq. (4) from the entrance to the outlet of the measuring-cell gives:

$$Y^*(H) = \frac{M^*}{N_{CO_2} u^*} H. \tag{5}$$

Eq. (5) clearly shows that in order to apply the dynamic method to measure solubility for each geometry of the measuring-cell, either the value Q^* or u^* must be determined. Otherwise, reported values of the solubility for systems cellulosic structure + solute + solvent can be smaller than the true value due to either very low (axial dispersion not negligible) or very large flow rates.

There is still a last question to discuss: if the composition of the extract changes appreciably during the CER period (the measuring period) then Y^* would be of very low significance for the design, except for the cases of fractional extraction, such as the SFE of caffeine [1] and carotenoids [14]. Therefore, the knowledge of the extract composition is required to completely characterize the pseudo-ternary system. Table 4 shows the phytochemical profile of the clove extract obtained in SFE_1. The major compounds were eugenol, β-caryophyllene, α-humulene and eugenyl acetate, regardless of the experimental condition. A similar behavior was observed for the clove extract obtained in SFE_2 (Table 5).

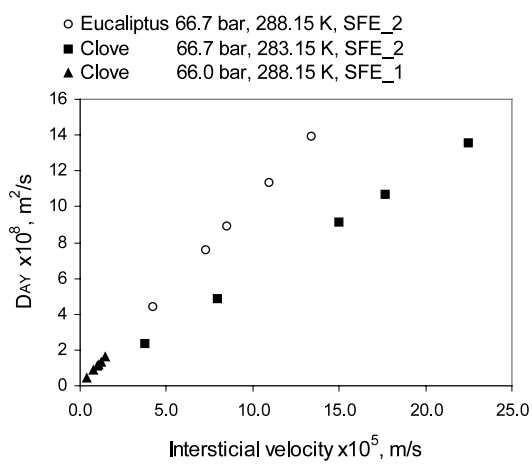

Fig. 6. Influence of raw material on the estimated value of D_{aY} as a function of the interstitial velocity.

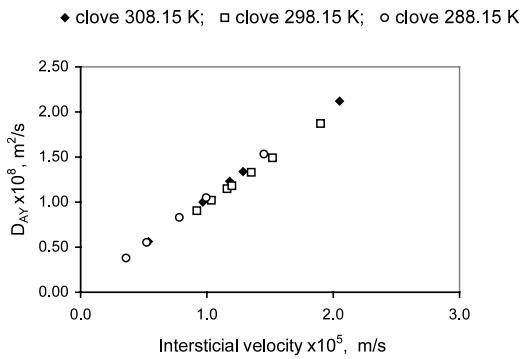

Fig. 7. Influence of temperature on the estimated value of D_{aY} at 100 bar as a function of the interstitial velocity, data from SFE_1.

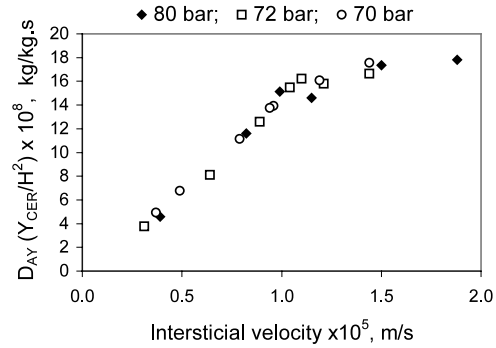

Fig. 8. Influence of the pressure on the axial dispersion term for the system clove buds /CO_2 (SFE_1) at 388.15 K.

Table 3
Solubility measured by the dynamic method for pseudo-ternary system

T K	P bar	$Y^* \times 10^3$ kg/kg	$Q^* \times 10^5$ kg/s	Experimental system
Clove				
283.15	66.7	258	1.84	SFE_2
288.15	66.0	220	1.74	SFE_1
288.15	66.7	234	1.85	SFE_2
288.15	70.0	230	1.51	SFE_1
288.15	72.0	238	1.65	SFE_1
288.15	80.0	244	1.60	SFE_1
288.15	100.0	277	1.64	SFE_1
298.15	100.0	267	1.65	SFE_1
308.15	100.0	230	1.54	SFE_1
Ginger				
293.15	150	5.15	1.57	SFE_3
293.15	200	4.14	1.63	SFE_3
293.15	250	5.38	1.64	SFE_3
303.15[a]	100	2.92	1.75	SFE_3
303.15	150	5.78	1.62	SFE_3
303.15	200	5.21	1.63	SFE_3
303.15	250	5.90	1.68	SFE_3
303.15[a]	300	6.57	1.70	SFE_3
313.15[a]	100	1.99	1.72	SFE_3
313.15	150	6.41	1.60	SFE_3
313.15	200	6.73	1.61	SFE_3
313.15	250	7.20	1.65	SFE_3
313.15[a]	300	5.97	1.72	SFE_3
Eucalyptus				
283.15	66.7	2.03	1.47	SFE_2
298.15	66.7	3.25	1.64	SFE_2
293.15	66.7	4.07	1.56	SFE_2
288.15	66.7	3.95	1.52	SFE_2
288.15	78.5	4.94	1.48	SFE_2

[a] Data for Ginger_2.

Table 4
Relative proportion for the compounds identified in the clove bud extract (SFE_1) at 100 bar 298.15 K and $Q^* = 1.65 \times 10^{-5}$ kg/s

Measuring time/60 s	Eugenol %	β-caryophyllene %	Eugenyl acetate %	Humulene %
Compounds				
10	58.38	23.24	16.01	2.37
20	59.93	21.64	16.35	2.08
30	59.87	20.26	17.86	2.01
40	60.74	19.55	17.71	2.00
50	62.28	19.16	16.67	1.89
60	63.63	17.28	17.25	1.84
70	64.19	16.36	17.77	1.65
80	66.65	13.98	17.90	1.47
90	69.31	12.96	13.36	1.37
120	72.03	10.92	15.61	1.44

Figs. 2 and 3 indicate that the CER period ends at about 50 min and so Tables 4 and 5 show that the composition of clove extracts remained approximately constant for measuring times smaller than 50 min. Therefore, although the origin of the raw material is important, for design purposes it can be overlooked. The quantitative analysis of the extract showed that the eugenol is present in larger amounts (larger mass) for all conditions. From this, one may suggest that the solubility for the pseudo-ternary system is governed by the solubility of the eugenol in CO_2. Table 6 shows the composition of the ginger extracts. Samples from the collector flask as well as from the capture column were analyzed and are identified as E1-CO_2 and E2-CO_2, respectively. The data show that Ginger_2 produced a richer extract as compared to Ginger_1 but the behavior of the solubility for both systems was similar (Table 3). Monteiro [25] showed that the composition of the ginger extracts remained approximately constant during the CER period and so the composition given in Table 6 corresponds to the ginger extract at any given processing time. Table 7 presents the composition of the eucalyptus extract (total). The substances present on larger amounts were aromadendrene, globulol and 1,8 cineol. About 25% of the sesquiterpenes were not identified for *E. tereticornis*, a plant easily grown in the Brazilian Northeast region, for which very few information is available in the literature to help to elucidate its composition.

A careful analysis of the data on Tables 4–7 show that care must be taken when using a global property to describe the behavior of a multicomponent mixture. Nevertheless, the use of a global property like Y^* to describe the thermodynamic restraints for systems such as vegetable material/

Table 5
Relative proportion for the compounds identified in the clove bud extract (SFE_2) at 66.67 bar 283 K and $Q^* = 1.47 \times 10^{-5}$ kg/s

Measuring time/60 s	Eugenol %	β-caryophyllene %	Eugenyl acetate %	Humulene %
Compounds				
10	60.27	25.52	11.68	2.53
15	59.57	24.37	13.44	2.62
45	63.59	20.34	13.69	2.37
60	64.28	19.63	13.78	2.31
85	66.90	16.96	13.57	1.78
105	65.54	17.10	15.24	2.10
155	83.63	6.11	10.26	0
165	80.18	8.25	11.58	0
332	91.25	2.61	6.10	0

Table 6
Relative proportion for the identified compounds (% area) in the ginger extracts

Substances	Ginger_1 (200 bar, 293.15 K)		Ginger_2 (100 bar, 303.15 K)		Ginger_2 (300 bar, 303.15 K)	
	E1-CO_2	E2-CO_2	E1-CO_2	E2-CO_2	E1-CO_2	E2-CO_2
Monoterpenes						
Camphene	2.75	–	1.68	0.63	1.04	tr
1,6-octadiene	5.60	–	–	–	–	–
β-myrcene	1.91	–	1.43	tr	0.93	tr
β-pinene	10.07	0.50	3.53	tr	2.19	tr
Limonene	3.60	–	–	–	–	–
β-phellandrene	–	–	2.40	tr	1.57	tr
Aromatic hydrocarbons						
m-diethyl-benzene	16.19	–	–	–	–	–
o-diethyl-benzene	10.06		–	–	–	–
Oxygenated monoterpenes						
1,8 Cineole	–	–	3.63	tr	2.29	tr
α-terpineol	–	–	0.37	0.35	0.34	tr
Citronelol	–	–	0.39	0.51	0.46	tr
Neral	0.93	1.01	4.42	3.45	4.03	2.95
Geraniol	–	–	0.65	0.68	0.62	tr
Geranial	1.55	1.73	11.26	8.72	10.45	7.35
Sesquiterpenes						
ar-curcumene	9.23	7.72	5.59	5.34	4.80	3.89
β-Selinene	–	–	tr	tr	tr	1.94
Caryophyllene	0.42	0.52	–	–	–	–
α-zingiberene	16.86	16.73	27.05	22.02	23.03	22.67
trans-guaiene	–	–	2.79	2.74	2.32	3.01
E,E-α-farnesene	9.17	8.92	11.52	14.80	9.58	8.41
β-bisabolene	–	–	4.73	tr	4.52	4.37
γ-cadinene	–	–	0.40	0.52	tr	tr
β-sesquiphellandrene	10.33	8.20	11.13	10.61	9.90	10.19
Sesquiterpenes non-identified	–	–	1.78	8.07	2.64	8.41
Gingerols						
Zingerol	1.13	4.31	–	–	–	–
cis-6-shogaol	–	1.02	–	–	–	–
trans-6-shogaol	0.75	5.14	–	–	–	–
6-gingerol	1.01	8.64	–	–	–	–
8-gingerol	–	2.39	–	–	–	–
methyl-8-gingerol	–	1.81	–	–	–	–
10-gingerol	–	3.80	–	–	–	–
Methyl-10-gingerol	–	0.94	–	–	–	–
Gingerols and Shogaols non-identified	–	7.90	tr	5.28	5.28	22.48
Others						
Farnesol	–	0.58	–	–	–	–
Palmitic acid	–	0.66	–	–	–	–
Nerolidol	–	–	1.09	1.38	0.91	1.46
2-undecanone	–	–	tr	0.27	tr	tr
Zingerone	–	–	2.45	7.67	8.63	2.87
1,10 di-epi-cubenol	–	–	0.71	1.00	0.67	tr
1-epi-cubenol	–	–	0.52	0.71	0.46	tr
Non-identified	0.44	17.48	0.48	4.81	3.34	–

Table 7
Relative proportion for the compounds identified in the eucalyptus extract (SFE_2) at 66.7 bar 288 K and $Q^* = 1.52 \times 10^{-5}$ kg/s

Substance	[% A]
para-cymene	1.03
Limonene	1.43
1.8-cineole	11.03
Gamma-terpinene	1.71
Alpha-fenchol	0.18
Trans-pinocarveol	0.31
4-terpineol	4.43
para-cumen-8-ol	0.58
cis-pinocarveol	0.81
alpha-terpineol	2.50
Para-cymen-4-ol	0.34
Carvacrol	0.46
Eugenol	1.45
Isoledene	0.25
1-tetradecene	0.26
α-gurjunene	1.72
trans-caryophyllene	1.89
β-gurjunene	0.83
Aromadendrene/α-guainene	21.07
allo-aromadendrene/seychellene	5.05
γ-gurjunene	0.33
β-selinene	0.64
α-selinene	1.76
γ-selinene	0.46
δ-cadinene	0.36
Globulol	13.83
Sesquiterpenes non-identified	25.29

CO_2 is convenient and can be used as long as there is no definite fractionation of the multicomponent mixture. In this situation, the system can be treated as a pseudo-ternary system. For a system such as residue from palm oil pressing/CO_2, the solubilities of fat acids, triglycerides and carotenoids in CO_2 are very different. In fact, the fat acids are much more soluble in CO_2 than the triglycerides and the carotenoids [14]. Such a system might require to be treated at least as a quaternary system [1].

4. Conclusions

The results have shown that the solubility for vegetable material systems (cellulosic structure + solute)/CO_2 can be treated as a pseudo-ternary system. The solubility of the solute in the solvent can be measured by the dynamic method using any type of measuring-cell geometry, as long as the critical solvent flow rate, Q^*, is determined. It is more convenient, from the experimental point of view, to keep the relationship between length and diameter of the measuring-cell as high as possible. The solubility, as expected, is a function of the raw material but not as strong as one might have guessed. Therefore, it is possible to use this type of data for design purposes. Certainly, for the majority of the processes, the choice would be to use solvent flow rates larger than Q^*. Nevertheless, the excess of solvent should be kept as low as possible to avoid the increase in operational costs, due to the increase in the solvent re-compression rate. For these calculations, the value of the solubility must be known and can be measure as proposed here. Zancan et al. [26], Povh et al. [27] and Rodrigues et al. [28] have demonstrated the usefulness of the solubility measured as proposed here to model the overall extraction curves of ginger, chamomile and anise seeds, using the Sovová model [21]. For an industrial process, the usage of solvent flow rates smaller than Q^* is justified for certain vegetable materials for which the solute is very hardly accessible by the solvent. As an example, it can be mentioned the extraction of certain ginger anti-oxidants that are located very internally into the solid particles [29].

Acknowledgements

The authors wish to express their gratitude to FAPESP (1995/05262-3 and 1999/01962-1) for the financial support. V.M. Rodrigues thanks FAPESP (1997/01241-7) for the Ph.D. assistantship. E.M.B.D. Sousa is grateful to DEQ–UFRN for the permission to develop her doctoral thesis. A.R. Monteiro thanks CAPES for the Ph.D. assistantship.

References

[1] G. Brunner, Gas Extraction: An Introduction to Fundamentals of Supercritical Fluids and the Application to Separation Processes, Springer, New York, USA, 1994.

[2] M.A. McHugh, V.J. Krukonis, Supercritical Fluid Extraction: Principles and Practice, Butterworth-Heinemann, Newton, USA, 1994.
[3] G. Vernin, E. Verinin, J. Metzger, L. Pujol, C. Parkanyi, GC/MS analysis of clove essential oils, in: George Charalambous (Ed.), Spices, Herbs and Edible Fungi, Elsevier Science, Amsterdam, Holland, 1994, p. 483.
[4] A.A. Craveiro, D.C. Queiroz, Óleos essenciais e química fina, Química Nova 16 (1993) 224.
[5] F.J.A. Matos, Farmácias Vivas, Edições da Universidade Federal do Ceará, Fortaleza, Brazil, 1998.
[6] J.P. Bartley, P. Foley, Supercritical fluid extraction of Australian-grown ginger (*Zingiber officinale*), Journal of the Science of Food and Agriculture 66 (1994) 365.
[7] A.R. Monteiro, M.A.A. Meireles, M.O.M. Marques, Ginger (*Zingiber officinale*) essential oil and oleoresin extraction with pressurized CO_2: an evaluation of pretreatment and process variables in oil composition, in: M. Perrut (ed.), Proceedings of the 5th Meeting on Supercritical Fluids: Natural Products and Materials, Nice, France, 2, 1998, p. 515.
[8] F.D. Brod, R. Oliveira, K.J. Park, Estudo de um secador convectivo de fluxo perpendicular e paralelo, Proceedings of the 29th Congresso Brasileiro de Engenharia Agrícola—CONBEA 2000, Fortaleza, CE, 2000, CD Rom.
[9] R. Gomide, in: Cenpro (Ed.), Manual de Operações Unitárias, São Paulo, Brazil.
[10] M.B. Jacobs, The Chemical Analysis of Food and Products, Robert Krieger Publishing Co., New York, USA, 1973.
[11] V.M. Rodrigues, M.A.A. Meireles, M.O.M. Marques, Determination of the solubility of clove essential oil in CO_2: a standardization of the dynamic method, Proceedings of the 5th International Symposium on Supercritical Fluids, Westin Atlanta, Georgia, USA, 2000, CD-Rom.
[12] S.R.S. Ferreira, M.A.A. Meireles, F.A. Cabral, Extraction of essential oil of black pepper with liquid carbon dioxide, Journal of Food Engineering 20 (1993) 121.
[13] E.M.B.D. Sousa, O. Chiavone-Filho, M.T. Moreno, H.N.M Oliveira, M.A.A. Meireles, Experimental results for the extraction of essential oil from the species *Lippia Sidoides* in pressurized carbon dioxide, Proceedings of the 2nd International Meeting on High Pressure Chemical Engineering, TUHH, Hamburg, Germany, 2001, CD-Rom.
[14] L.F. França, M.A.A. Meireles, Modeling the extraction of carotene and lipids from pressed palm oil (*Elaes guineensis*) fibers using supercritical CO_2, Journal of Supercritical Fluids 18 (2000) 35.
[15] A.R. Monteiro, M.A.A. Meireles, M.O.M. Marques, A.J. Petenate, Extraction of the soluble material from the shells of the bacuri fruit (*Platonia insignis* Mart) with pressurized CO_2 and other solvents, Journal of Supercritical Fluids 11 (1997) 91.
[16] F.W. McLaferty, D.B. Stauffer, The Wiley/NBS Registry of Mass Spectral Data, vols. 1–2, John Wiley and Sons, New York, USA, 1989.
[17] R.P. Adams, Identification of Essential Oil Components by Gas Chromatography/Mass Spectroscopy, Allured Publishing Corporation, Illinois, USA, 1995.
[18] C.H. Collins, G.L. Braga, P.S. Bonato, Introdução a Métodos Cromatográficos, Editora da Unicamp, Campinas, Brazil, 1995.
[19] F.J.A. Matos, Introdução à Fitoquímica Experimental, Editora da Universidade Federal do Ceará, Fortaleza, CE, Brazil, 1997.
[20] R.J. Freund, R.C. Littell, SAS System for Regression—SAS Series in Statistical Applications, SAS Institute Inc., NC, USA, 1995.
[21] H. Sovová, Rate of the vegetable oil extraction with supercritical CO_2–I. Modeling of extraction curves, Chemical Engineering Science 49 (1994) 409.
[22] E. Santacesaria, M. Morbidelli, A. Servida, G. Storti, S. Carrà, Separation of xylenes on Y zeolites. 2. Breakthrough curves and their interpretation, Ind. Eng. Chem. Proc esso Des. Dev. 21 (1982) 446.
[23] O.J. Cathpole, R. Berning, M.B. King, Measurement and correlation of Packed-Bed axial dispersion coefficients in supercritical carbon dioxide, Ind. Eng. Chem. Res. 35 (1996) 824.
[24] C.-S. Tan, D.-C. Liou, Axial dispersion of supercritical carbon dioxide in packed beds, Ind. Eng. Res. 28 (1989) 1246.
[25] A.R. Monteiro, Extração do Óleo Essencial/Oleoresina de Gengibre (*Zingiber officinale* Roscoe) com CO_2 Supercrítico: uma avaliação do pré-tratamento e das variáveis de processo, Doctoral thesis, FEA—Universidade Estadual de Campinas (Unicamp), Campinas, São Paulo, Brazil, 1999.
[26] K.C. Zancan, M.O.M. Marques, M.A.A. Meireles, A.J. Petenate, Extraction of ginger (*Zingiber officinale* Roscoe) oleoresin with CO_2 and Co-solvents: a study of the antioxidant action of the extracts, Proceedings of the 2nd International Meeting on High Pressure Chemical Engineering, TUHH, Hamburg, Germany, 2001, CD-Rom.
[27] N.P. Povh, M.A.A. Meireles, M.O.M. Marques, Supercritical CO_2 extraction of essential oil and oleoresin from chamomile (*Matricaria recutita* [L.] Rauschert), Proceedings of the 2nd International Meeting on High Pressure Chemical Engineering, TUHH, Hamburg, Germany, 2001, CD-Rom.
[28] V.M. Rodrigues, M.O.M. Marques, M.A.A. Meireles, Supercritical extraction of essential oil from anise seed (*Pimpinella anisum*, L) using CO_2: Kinetics and equilibrium data, Proceedings of the 2nd International Meeting on High Pressure Chemical Engineering, TUHH, Hamburg, Germany, 2001, CD-Rom.
[29] V.S. Govidarajan, CRC Critical Reviews in Food Science and Nutrition, vol. 17, CRC Press Inc., Florida, 1982, p. 1.